Attenuated anticorrelation between the default and dorsal attention networks with aging: evidence from task and rest

R. Nathan Spreng [a,b,*,1], W. Dale Stevens [c,**,1], Joseph D. Viviano [c], Daniel L. Schacter [d]

[a] Laboratory of Brain and Cognition, Department of Human Development, Cornell University, Ithaca, NY, USA
[b] Human Neuroscience Institute, Cornell University, Ithaca, NY, USA
[c] Cognition and Aging Neuroscience Laboratory, Department of Psychology, York University, Toronto, Ontario, Canada
[d] Department of Psychology, Harvard University, Cambridge, MA, USA

ARTICLE INFO

ABSTRACT

Anticorrelation between the default and dorsal attention networks is a central feature of human functional brain organization. Hallmarks of aging include impaired default network modulation and declining medial temporal lobe (MTL) function. However, it remains unclear if this anticorrelation is preserved into older adulthood during task performance, or how this is related to the intrinsic architecture of the brain. We hypothesized that older adults would show reduced within- and increased between-network functional connectivity (FC) across the default and dorsal attention networks. To test this hypothesis, we examined the effects of aging on task-related and intrinsic FC using functional magnetic resonance imaging during an autobiographical planning task known to engage the default network and during rest, respectively, with young (n = 72) and older (n = 79) participants. The task-related FC analysis revealed reduced anticorrelation with aging. At rest, there was a robust double dissociation, with older adults showing a pattern of reduced within-network FC, but increased between-network FC, across both networks, relative to young adults. Moreover, older adults showed reduced intrinsic resting-state FC of the MTL with both networks suggesting a fractionation of the MTL memory system in healthy aging. These findings demonstrate age-related dedifferentiation among these competitive large-scale networks during both task and rest, consistent with the idea that age-related changes are associated with a breakdown in the intrinsic functional architecture within and among large-scale brain networks.

© 2016 Elsevier Inc. All rights reserved.

1. Introduction

Anticorrelation between large-scale brain networks is a central feature of human functional brain organization (e.g., Fox et al., 2005; Fransson, 2005; Golland et al., 2008). Anticorrelation is observed as positive within-network functional connectivity (FC) concomitant with negative between-network FC of the dorsal attention and default networks (Fox et al., 2005). The dorsal attention network is composed of the frontal eye fields (FEF), the ventral frontal region precentral ventral (PrCv), middle temporal motion complex (MT+), inferior parietal sulcus (IPS), superior parietal lobule (SPL), and dorsolateral prefrontal cortex (DLPFC). Regions of the default network include medial prefrontal cortex (MPFC), posterior cingulate cortex (PCC), superior and inferior frontal gyrus, lateral temporal lobes, inferior parietal lobule (IPL), and the medial temporal lobes (MTLs; Fox et al., 2005), although there is evidence that the MTL may have a unique functional relationship with the default network (Eldaief et al., 2011; Ward et al., 2014) and comprises subregions that have dissociable patterns of FC (Kahn et al., 2008). The dorsal attention and default networks are inversely engaged during externally and internally directed cognition, respectively (Spreng et al., 2010a), and this reciprocal pattern of activity may serve as a critical neural substrate for flexibly allocating attentional resources and is important for healthy cognitive function (Whitfield-Gabrieli and Ford, 2012). Magnitude of anticorrelation is associated with externally directed task performance in young adults (e.g., Hampson et al., 2010).

Numerous age-related changes are apparent in brain activation during externally oriented attention (Spreng et al., 2010b), which reliably engages the dorsal attention network in the young (Gusnard et al., 2001; Spreng et al., 2010a). In addition, reductions

* Corresponding author at: Laboratory of Brain and Cognition, Department of Human Development, Cornell University, Martha Van Rensselaer Hall, Room G62C, Ithaca, NY 14853, USA. Tel.: 607-255-4396; fax: 607-255-9856.
** Corresponding author at: Department of Psychology, Sherman Health Science Research Centre, York University, 281 Ian Macdonald Blvd., Toronto, ON M3J 1P3, Canada. Tel.: 416-736-2100 x44662; fax: 416-736-5814.
E-mail addresses: nathan.spreng@gmail.com (R.N. Spreng), stevensd@yorku.ca (W.D. Stevens).
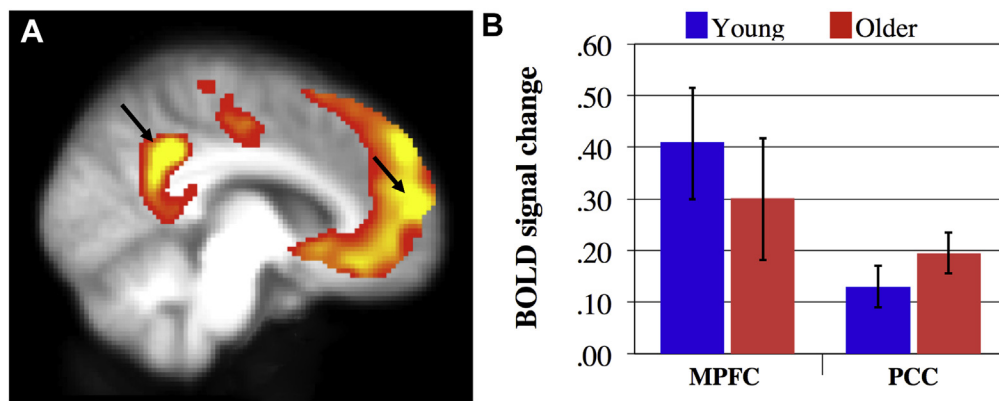[1] Equal contribution.

Fig. 1. Autobiographical planning task activation. (A) Young and older adults robustly engaged the default network during autobiographical planning, relative to visuospatial planning (see Spreng and Schacter, 2012). (B) MPFC and PCC (see arrows) activity was significantly elevated relative to fixation baseline in both young (t_{MPFC} (17) = 3.89, $p < 0.001$; t_{PCC} (17) = 3.26, $p < 0.005$) and older adults (t_{MPFC} (16) = 2.56, $p < 0.05$; t_{PCC} (17) = 3.80, $p < 0.001$). No differences were observed in the magnitude of MPFC or PCC activation between groups (t_{MPFC} (33) = 0.69, ns; t_{PCC} (34) = 1.00, ns). Differences between groups in the connectivity profile thus cannot be attributed to differences in task-related brain activity. Abbreviations: MPFC, medial prefrontal cortex; PCC, posterior cingulate cortex.

in task-related default network suppression and altered FC have been observed with advancing age (Andrews-Hanna et al., 2007; Damoiseaux et al., 2008; Grady et al., 2010; Hafkemeijer et al., 2012; Sala-Llonch et al., 2012; Sambataro et al., 2010; Stevens et al., 2008; Turner and Spreng, 2015). These findings complement whole-brain resting-state FC (RSFC) observations of a dedifferentiation of network connectivity with age, with increases in RSFC between large-scale brain systems in older adults (Betzel et al., 2014; Chan et al., 2014; Geerligs et al., 2015; Grady et al., 2016; Meunier et al., 2009; Onoda and Yamaguchi, 2013). It is unclear, however, if the robust pattern of anticorrelated activity between the default and dorsal attention networks is preserved into older adulthood.

Chan et al. (2014) observed increased correlations between default and dorsal attention networks as one feature of a larger pattern of reduced network segregation in older adulthood (see also, Grady et al., 2016). However age-related changes in anticorrelation between networks were not investigated in this study. Reduced anticorrelations between default and dorsal attention networks have been reported in older adults (Betzel et al., 2014; Wu et al., 2011). However, the use of mean global signal regression (GSR) in these studies may have altered the interregional correlation differences between groups (Murphy et al., 2009; Saad et al., 2012) complicating the interpretation of negative correlation values (Gotts et al., 2013). More recently, preprocessing procedures that do not rely on GSR have revealed that the antagonism between medial and lateral prefrontal cortex is attenuated in older adults (Keller et al., 2015), but age-related changes in anticorrelation between the dorsal attention and default networks more broadly have not been reported.

Consistent with the critical role of the MTL in episodic memory (Squire et al., 2004) and the marked deficits in episodic memory in age-related dementia, several studies have demonstrated reduced RSFC of the MTL in particular with other default network regions in individuals with mild cognitive impairment (Das et al., 2013, 2015; Jin et al., 2012), and Alzheimer's disease (for review see Hafkemeijer et al., 2012; Mevel et al., 2011), including patients in prodromal stages (Sperling et al., 2010; Wang et al., 2006). Episodic memory also shows declines in typical healthy aging (Grady, 2012), and there is evidence for MTL-cortical reductions in FC at rest with advancing age (Salami et al., 2014). An earlier study, however, found that while some subsystems of the default network showed differential patterns of RSFC between young and older adults, the MTL subsystem in particular, did not show any age-related

differences (Campbell et al., 2013). Therefore, the extent to which FC of the MTL is altered in aging and potentially related to decline in memory remains unclear.

Spreng and Schacter (2012) assessed patterns of large-scale network activity in young and older adults during performance of an autobiographical planning task that engages the default network and a visuospatial planning task (the Tower of London) that engages the dorsal attention network (Spreng et al., 2010a), consistent with the anticorrelated domains of internalized and externalized cognition. Older adults robustly engaged the default network during the autobiographical planning task, not different in magnitude than their younger counterparts (Spreng and Schacter, 2012, see also Fig. 1). Unlike young adults, older adults had reduced suppression of the default network during visuospatial planning (Spreng and Schacter, 2012; Turner and Spreng, 2015). Thus, autobiographical planning provides a unique opportunity to examine FC patterns in older adults, and potential age-related changes in anticorrelation during a task known to engage the default network, without the confound of age-related differences in task-based activation patterns. In the present study, we examine (1) the impact of age on task-related MPFC connectivity during autobiographical planning using a multivariate FC analysis and (2) patterns of RSFC in young and older adults, leveraging a preprocessing strategy that does not involve GSR. Together these analyses provide the first evidence that aging is associated with reduced anticorrelation between the default and dorsal attention networks during task and rest and decreased intrinsic FC of the MTL across both networks.

2. Methods

2.1. Participants

All participants were healthy, with normal or corrected-to-normal visual acuity, and no history of psychiatric, neurologic, or other medical illness that could compromise cognitive functions. All participants gave written informed consent in accordance with the Harvard Institutional Review Board or the Human Subjects Research Committee at Massachusetts General Hospital.

2.1.1. Experiment 1

Task functional magnetic resonance imaging (fMRI) data were collected from 18 young adults (mean age = 22.8 ± 2.4 years; range = 19–27; 9 women) and 18 older adults (mean age = 71.4 ± 4.0 years; range = 63–78; 9 women) previously reported

by Spreng and Schacter (2012). Years of education were equivalent between groups (young = 15.9 ± 1.9 years; older = 15.9 ± 1.1 years). Older adults were high functioning, with a healthy mental status (Mini–Mental Status Examination ≥27; mean = 28.4 ± 1.5), and not depressed (Geriatric Depression Scale ≤3.0; mean = 0.8 ± 0.9). Most participants were right-handed; one male in each group was left-handed. One older adult was excluded due to outlier MPFC blood-oxygen-level dependent (BOLD) signal activation >5 standard deviations (SDs) from the group mean.

2.1.2. Experiment 2

Resting-state fMRI data were collected from an independent sample of 54 young adults (mean age = 24 ± 3.8 years; range = 18–35; 27 women) and 61 older adults (mean age = 74.6 ± 3.8 years; range = 65–86; 31 women). Years of education were equivalent between groups (young = 16 ± 2.1 years; older = 16 ± 2.8 years). These older adults were high functioning, with a healthy mental status (Mini-Mental Status Examination ≥ 25; mean = 28.86 ± 1.2), and not depressed (Geriatric Depression Scale ≤ 4; mean = 0.7 ± 0.9).

2.2. Procedure

2.2.1. Experiment 1–task

The autobiographical planning task required participants to devise plans to meet specific goals in their personal futures. For example, "exercise" constituted one of the goals in the autobiographical planning task. Participants viewed the goal and then saw 2 steps they could take toward achieving that goal ("make routine" and "walk more") and an obstacle they needed to overcome to achieve the goal ("avoid injury"). They were instructed to integrate the steps and obstacles into a cohesive personal plan that would allow them to achieve the goal. Participants completed 24 autobiographical planning trials. The pacing of the task was such that the goal was presented for 5 seconds, followed by 20 seconds of plan formation where the goal, steps, and obstacle were visible.

2.2.2. Experiment 2–rest

Participants were instructed to fixate on a centrally presented crosshair while blinking and breathing normally, to remain motionless, and to not fall asleep. Compliance was confirmed by verbal confirmation at the end of each run.

2.3. MRI data collection and preprocessing

2.3.1. Experiment 1

Brain imaging data were acquired at the Harvard Center for Brain Sciences with a 3.0 T Siemens TimTrio MRI scanner with a 32-channel head coil. Anatomical scans were acquired using a T1-weighted multiecho volumetric MRI (repetition time [TR] = 2530 ms; echo time [TE's] = 1.64, 7.22 ms; 7° flip angle; 1.0-mm isotropic voxels). Six 7-min task BOLD functional scans were acquired with a T2*-weighted echo planar imaging pulse sequence (TR = 2500 ms; TE = 30 ms; 85° flip angle; 39 axial slices parallel to the plane of the AC-PC; 3.0 × 3.0 × 2.5-mm voxels with a 0.5-mm gap).

Task fMRI data were preprocessed using SPM2 (Wellcome Department of Cognitive Neurology, London, UK). The first 4 volumes in each run were excluded from analyses to allow for T1-equilibration effects. Data were corrected for slice-dependent time shifts and for head motion within and across runs using a rigid body correction. During the autobiographical planning blocks, no differences in head motion were observed between younger and older adults in the 6 motion parameters (F (5,30) = 0.94, p = 0.472). The data were then normalized to a combined young-older brain template that approximated Montreal Neurological Institute (MNI)

atlas space to compare brain data across age groups (Buckner et al., 2004). The volumetric time series was then resampled at 2-mm cubic voxels and spatially smoothed with an 8-mm full-width-at-half-maximum Gaussian kernel.

2.3.2. Experiment 2

All brain imaging data were acquired at the Athinoula A. Martinos Center for Biomedical Imaging, Massachusetts General Hospital (Charlestown, MA, USA) on a 3.0 T Siemens Magnetom TimTrio MRI scanner with a 12-channel head coil (Siemens Medical Solutions, Erlangen, Germany). Anatomical images were acquired using a high-resolution 3-dimensional magnetization-prepared rapid gradient echo sequence (MPRAGE: 128 sagittal slices; TR = 2530 ms; TE = 3.45 ms; flip angle = 7°; voxel size = 1 × 1 × 1.33 mm). For one sample of young (n = 37) and older (n = 41) adults, functional images for 4 rest runs were collected using T2*-gradient echo, echo-planar imaging sensitive to BOLD contrast (TR = 2500 ms; TE = 30 ms; flip angle = 90°; voxel size = 4-mm isotropic) in 4 sets of 112 volumes per run acquired axially in 36 slices, yielding whole-brain coverage, for a total of 448 volumes (duration = 18 minutes 40 seconds). For a second sample of young (n = 18) and older (n = 32) adults, functional images for 2 rest runs were collected using T2*-gradient echo, echo planar imaging sensitive to BOLD contrast (TR = 2500 ms; TE = 30 ms; flip angle = 90°; voxel size = 3-mm isotropic) in 2 sets of 124 volumes per run acquired axially in 36 slices with a 0.5-mm gap between slices, yielding whole-brain coverage, for a total of 248 volumes (duration = 10 minutes 20 seconds). To maximize statistical power, all young adults were combined and all older adults were combined to form 2 groups of large sample sizes (young: n = 55; older: n = 73) for all RSFC analyses.

Echo-planar images were preprocessed using the Analysis of Functional Neuroimages software package (Cox, 1996). For each run, the first 4 image-volumes were removed to allow for T1-equilibration effects. Large transients in the remaining volumes were removed through interpolation (3dDespike). Volumes were then slice-time corrected (3dTshift) and coregistered to the volume nearest the anatomical scan (3dVolreg). In RSFC analyses, artifacts in the data resulting from participant head motion are particularly problematic, especially when comparing samples across different populations (Power et al., 2012; Satterthwaite et al., 2012; Van Dijk et al., 2012). Numerous data analysis techniques have been developed to address this potential problem; one approach involves a combination of GSR and censoring of volumes coinciding with periods of abrupt and/or excessive motion, known as "scrubbing" (Power et al., 2014). However, a number of studies have demonstrated that GSR can distort the results of RSFC analyses in several ways (Gotts et al., 2013; Murphy et al., 2009; Saad et al., 2012) and introduce spurious anticorrelations (Murphy et al., 2009). Scrubbing can involve discarding a substantial portion of data, often unevenly across groups, thus resulting in a loss of statistical power and the potential introduction of group confounds (Satterthwaite et al., 2013). A particularly effective approach to the removal of nuisance physiological, nonphysiological, and motion-related artifacts is the ANATICOR procedure (Jo et al., 2010). This approach has been shown to drastically reduce or virtually eliminate motion-related artifacts in resting-state time-series analyses (Jo et al., 2013). Furthermore, the method eschews temporal filtering (e.g., bandpass filtering), which is ineffective at removing signals with frequencies above the Nyquist frequency (i.e., 0.5 × 1/TR = 0.2 Hz in the present study), such as cardiac and respiratory signals (Gotts et al., 2013; Van Dijk et al., 2010), and GSR, which can distort RSFC results in a number of detrimental ways (Gotts et al., 2013; Murphy et al., 2009; Saad et al., 2012). A modified version of the ANATICOR procedure was used here, as described previously (Fischl et al., 2002; Stevens et al., 2015). For each subject, the anatomical

scan was segmented into tissue compartments using Freesurfer (Fischl et al., 2002). Then, ventricle, white-matter, and draining-vessel masks were created and eroded to prevent partial volume effects with gray matter. These masks were then applied to the volume-registered echo-planar image yielding pure nuisance time series for the ventricles and draining-vessels, as well as local estimates of the white-matter BOLD signal averaged within a 15-mm radius sphere. To summarize, nuisance variables for each voxel's time-series included: an average ventricle time-series, an average draining-vessel time-series, a local average white-matter time-series, 6 head motion parameter estimates, and the temporal derivative of each of the latter. All of the above nuisance time-series were detrended with fourth-order polynomials. Least-squares model fitted time-series of these nuisance variables were then subtracted from the voxel time-series yielding a residual time-series that was used in all subsequent statistical analyses. To compare the differential effects of preprocessing techniques, we also analyzed the resting-state data using GSR combined with the scrubbing technique (GRS + Scrubbing) described by Power et al. (2012). Briefly, framewise displacement (FD: sum of absolute values of the differentials of the 3 translational and 3 rotational motion parameters) and signal change (DVARS) were calculated, and any volumes with FD > 0.3 mm or DVARS > 0.3%, as well as the 2 preceding and 2 following volumes, were discarded from the time series. Only participants with at least 120 volumes remaining after scrubbing were included in the group analyses, resulting in 54 young and 34 older adults for this analysis. Finally, for both analyses, the volumetric time series was then smoothed with a 6-mm full-width-at-half-maximum Gaussian kernel (3dBlurInMask), then normalized to the Analysis of Functional Neuroimages MNI_152 atlas space and resampled at 3-mm isotropic (3dAllineate).

2.4. Task-related FC

The preprocessed autobiographical planning data from experiment 1 were analyzed with seed partial least squares (PLS, Krishnan et al., 2011; McIntosh, 1999). Seed PLS is a data-driven multivariate statistical technique that reveals functional activity across the entire brain that correlates with activity in a seed region. The covariance between activity in the seed and all other brain voxels is decomposed into latent variables (LVs) that can identify multiple patterns of FC. The advantage of block seed PLS is that potential movement confounds associated with age are substantially reduced. Furthermore, the decomposition and associated resampling techniques consider all voxels simultaneously, thus avoiding the problem of multiple statistical comparisons. Because of its ability to identify groups of brain regions with covarying FC, this technique is methodologically suited to the investigation of large-scale brain networks. In 2-seed PLS analyses, activity was extracted from 2 regions of interest (ROI; peak voxel plus 26 neighboring voxels) centered on the location of peak activation within the MPFC and PCC (MNI coordinates: −4, 62, 14 and −10, −48, 36, respectively) during autobiographical planning (Fig. 1) and correlated across participants with all other brain voxels; PLS then was used to identify patterns of correlation that differed between young and older adults. Significance of the LVs was determined by 2500 permutation tests, using resampling without replacement. Reliability of each voxel's contribution to an LV across participants was calculated by a bootstrap procedure that resampled the data 500 times, with replacement, to estimate the standard error of the weight of each voxel on the LV. A bootstrap ratio, calculated as the ratio of each weight to its standard error, was thresholded at ± 1.96, equivalent to $p < 0.05$. For each participant, a composite brain score was calculated that provides an index of how strongly each participant expresses the pattern of activity identified by that LV. To

examine differences in connectivity across groups, the correlation between these scores from each significant LV and the seed values was calculated. Confidence intervals (95%) were calculated from the bootstrap, and differences between groups were determined via a lack of overlap in these confidence intervals. In a set of auxiliary analyses, we found that the observed pattern of FC was not related to measures of gray- and white-matter atrophy (see supplemental material).

In a complementary ROI-based analysis, we next extracted BOLD signal from 6 ROIs of the dorsal attention network and 6 ROIs of the default network defined in an independent study delineating the brain's large-scale networks in 1000 adults (Yeo et al., 2011). For each group, the between-subjects cross-correlation matrix was determined. See Table 1 for all seed region coordinates.

2.5. Intrinsic FC

To analyze whole-brain patterns of intrinsic low-frequency BOLD correlations and assess their differences by age, the mean BOLD signal timecourse was extracted from spherical seed ROIs with 6-mm radii centered on the location of peak activation within the MPFC and PCC during autobiographical planning (Fig. 1). The correlation coefficient for each seed's timecourse with the timecourse for every other voxel in the brain was computed using Pearson's product-moment formula. These values were then converted to z-values using Fisher's r-to-z transformation. The whole-brain voxel-wise z-map was then subjected to random effects analyses to assess statistical significance across participants at the group level using t-tests (threshold: $q < 0.05$, false discovery rate corrected). ROI-based analyses were then used to further explore age-related differences in within- and between-network RSFC among a set of critical nodes of both the dorsal attention and default networks. For each of 6 nodes within each network (Table 1), a spherical ROI with a radius of 6 mm was centered on the a priori coordinate based on previous literature as discussed previously (Yeo et al., 2011). The pairwise RSFC of each node with every other node, both within and between the 2 networks, was calculated, and random effects analyses were used to assess age-related differences in within- and between-network FC.

3. Results

3.1. Whole-brain task-related FC

The task-related FC analysis, using the MPFC as a seed region, yielded 2 statistically significant LVs depicting qualitatively different FC patterns that differentiated the 2 age groups. One LV showed significant and reliable MPFC connectivity in the young, but not the older adults, accounting for 43.9% of the variance in the data ($p < 0.05$). We observed positive connectivity of the MPFC with the default network, and conversely, negative connectivity with the dorsal attention network (Fig. 2A), demonstrating the expected pattern of anticorrelation. The other LV showed significant and reliable MPFC connectivity in the older (r = 0.84) but not the young (r = -0.14) adults, accounting for 56.1% of the variance in the data ($p < 0.05$). We observed diffuse positive connectivity of the MPFC with the default network, key regions of the dorsal attention network, and other regions (Fig. 2B). Multivariate patterns of connectivity were not significant for the PCC ($p = 0.18$).

3.2. ROI-based task-related FC

We next investigated between-subject correlations among critical nodes of the dorsal attention and default networks based on coordinates from previous literature (Yeo et al., 2011). Correlation

Table 1
Age by network connectivity interactions

Network	ROI	Coordinates (x, y, z)	GSR + Scrubbing				ANATICOR			
			Interaction	Crossover	F-stat	*p*-value	Interaction	Crossover	F-stat	*p*-value
Both	All		✓	✓	32.85	<0.001	✓	✓	16.45	<0.001
Dorsal attention	All		✓	✓	24.43	<0.001	✓	✓	9.50	<0.01
Default	All		✓	✓	23.63	<0.001	✓	✓	15.37	<0.001
Dorsal attention	FEF	−22, −8, 54	✓	✓	13.99	<0.001	✓	✓	4.59	<0.05
	IPS	−34, −38, 44	✓	✓	21.88	<0.001	✓	✓	8.26	<0.01
	SPL7a	−18, −69, 51	✓	✓	12.30	<0.001	✓	✓	4.76	<0.05
	MT+	−51, −64, −2	✓		12.90	<0.001			3.69	n.s.
	SPL7p	−8, −63, 57			2.41	n.s.			0.68	n.s.
	PrCv	−49, 3, 34	✓	✓	26.42	<0.001	✓	✓	12.30	<0.001
Default	PFCdp	−27, 23, 48	✓	✓	16.24	<0.001	✓	✓	10.91	<0.001
	IPL	−41, −60, 29	✓	✓	16.37	<0.001	✓	✓	9.84	<0.01
	STS	−64, −20, −9			0.85	n.s.			1.22	n.s.
	MPFC	−7, 49, 18	✓	✓	26.82	<0.001	✓	✓	19.73	<0.001
	PCC	−7, −52, 26	✓	✓	18.62	<0.001	✓	✓	11.43	<0.001

Interactions: significant age (young vs. older) × differentiation (within- vs. between-network RSFC) interaction; crossover, significant crossover interaction.
Key: FEF, frontal eye fields; GSR, global signal regression; IPL, inferior parietal lobule; IPS, inferior parietal sulcus; MPFC, medial prefrontal cortex; MT+, middle temporal area complex; n.s., not significant; PCC, posterior cingulate cortex; PFCdp, posterior dorsolateral prefrontal cortex; PrCv, ventral precentral sulcus; ROI, regions of interest; SPL7a, anterior superior parietal lobule; SPL7p, posterior superior parietal lobule; STS, superior temporal sulcus. Parahippocampal cortex (PHC) coordinate: −25, −32, −18.

patterns were consistent with the MPFC whole-brain connectivity results. Younger adults showed high positive within network connectivity, and negative between network connectivity, consistent with the predicted anticorrelation pattern between these networks (Fig. 3). A notable exception is the PrCv connectivity with the default network, likely due to the motor demands of the autobiographical planning task (button press response). In contrast, task-based FC for the older adults showed a dedifferentiated correlation pattern (Fig. 3).

3.3. Whole-brain intrinsic FC

First, the GSR + Scrubbing RSFC analysis revealed the expected pattern of anticorrelations between the default and dorsal attention networks broadly in both young and older adults, when seeding both the MPFC and PCC, with older adults showing decreased within network and increased between network RSFC relative to young adults (Figs. 4A–C, 5A–C). However, as discussed previously, GSR can introduce spurious negative correlations and
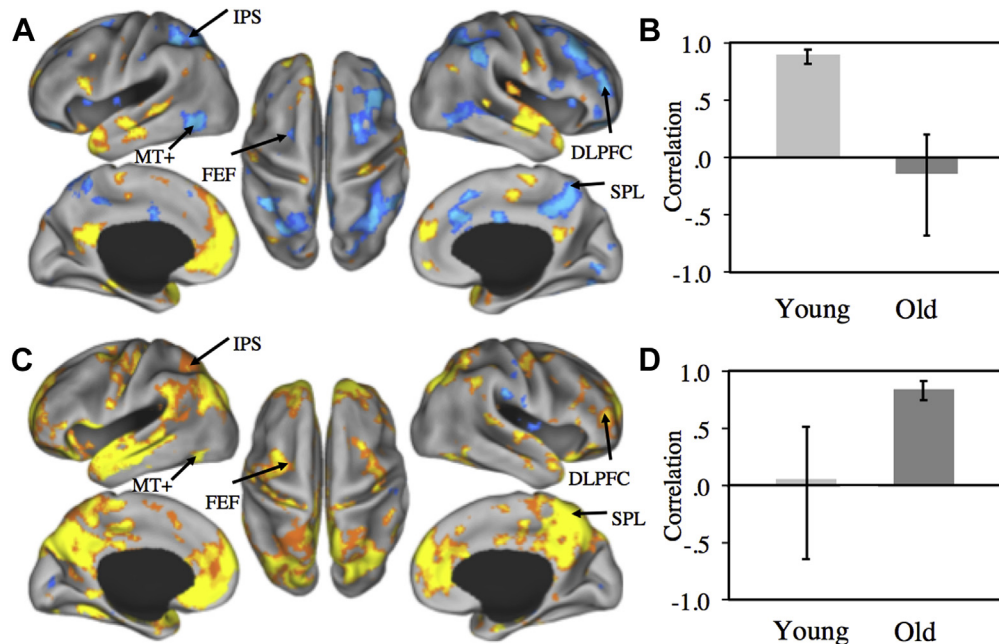

Fig. 2. Patterns of positive and negative correlations with the MPFC. (A) Regions functionally connected with the MPFC during autobiographical planning in young adults only. (C) Regions functionally connected with the MPFC in the older adults only. Correlations (B, D) represent the association between the MPFC seed activity and a composite brain activity score across participants within each group. The magnitude of correlation between MPFC and the activity represented in (A) was higher in the young than older adults (the correlation in the older adults did not differ from zero). The magnitude of correlation between the MPFC and the activity represented in (C) was higher in the older than young adults (the correlation in the young adults did not differ from zero). The pattern of functional connectivity in young adults demonstrates high within network and negative between network correlations, consistent with default-dorsal attention network anticorrelation. However, task-related functional connectivity in the older adults shows a qualitatively different pattern, with positive connectivity in FEF, MT+, IPS, SPL, and DLPFC—a network of regions comprising the dorsal attention network and anticorrelated with the default network in the young. Warm colors indicate positive correlations; cool colors depict negative correlations. Abbreviations: DLPFC, dorsolateral prefrontal cortex; FEF, frontal eye fields; IPS, inferior parietal sulcus; MPFC, medial prefrontal cortex; MT+, middle temporal area complex; SPL, superior parietal lobule. (For interpretation of the references to color in this figure legend, the reader is referred to the Web version of this article.)
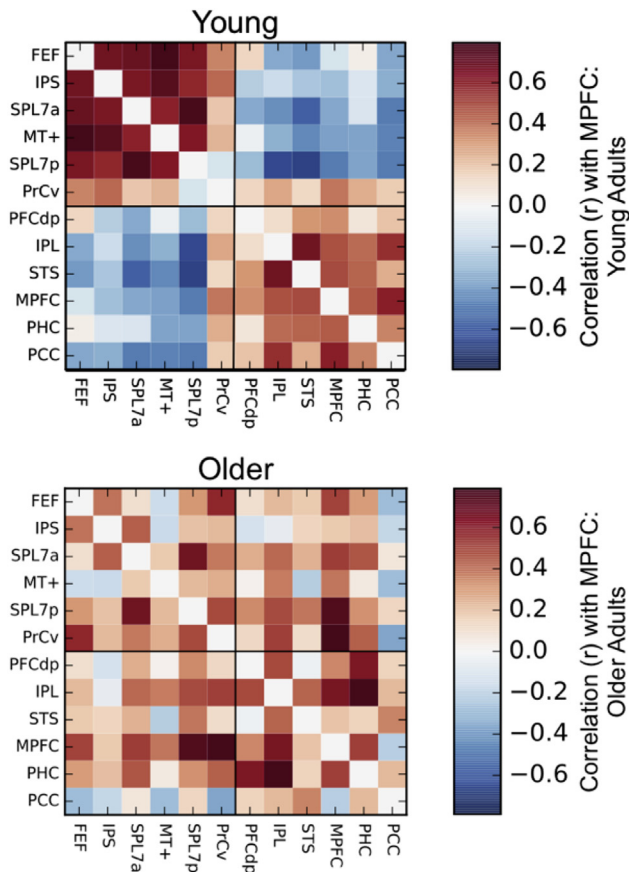
Fig. 3. Nodewise task-related FC of the MPFC in young versus older adults. In young adults (top row), activity in the MPFC is coupled with other regions of the default network (warm colors) during autobiographical planning and anticorrelated with only dorsal attention network regions (cool colors). In older adults (bottom row), the MPFC shows undifferentiated coupling with most nodes of both the default and dorsal attention networks (warm colors). See Table 1 node labels and coordinates. Abbreviations: FC, functional connectivity; FEF, frontal eye fields; IPL, inferior parietal lobule; IPS, inferior parietal sulcus; MPFC, medial prefrontal cortex; MT+, middle temporal area complex; PCC, posterior cingulate cortex; PFCdp, posterior dorsolateral prefrontal cortex; PrCv, ventral precentral sulcus; SPL7a, anterior superior parietal lobule; SPL7p, posterior superior parietal lobule; STS, superior temporal sulcus. (For interpretation of the references to color in this figure legend, the reader is referred to the Web version of this article.)

distort RSFC data in other ways (Gotts et al., 2013; Murphy et al., 2009; Saad et al., 2012), thus, our interpretations are based on our primary analysis which used the ANATICOR procedure without GRS + Scrubbing. As expected, anticorrelations between the dorsal attention and default networks were reduced in magnitude and more circumscribed. Nevertheless, this analysis provided a consistent and convergent pattern of results with the task driven analysis. The MPFC showed strong positive RSFC with the default network broadly, and negative correlations with the dorsal attention network, including the FEF, PrCv, MT+, IPS, SPL, and DLPFC in the young adults (Fig. 4D). The older adults showed a similar pattern of MPFC RSFC but with robustly attenuated anticorrelation with dorsal attention network regions (Fig. 4E). A direct comparison between the young and older adults (Fig. 4F) demonstrated reduced RSFC of the MPFC with other default network regions (PCC, IPL, MTL, lateral temporal cortex, including the superior temporal sulcus, and superior frontal gyrus) and reduced anticorrelation with dorsal attention network regions (PrCv, IPS, SPL, and right DLPFC). RSFC analyses of the PCC showed a highly similar pattern of results as for the MPFC (Fig. 5), with the

older adults showing substantially reduced RSFC with the majority of the default network (MPFC, superior temporal sulcus, superior frontal gyrus, IPL, and MTL), and reduced anticorrelation with all nodes of the dorsal attention network (FEF, PrCv, MT+, IPS, SPL, and DLPFC; Fig. 5F). All RSFC maps are displayed at a threshold of q < 0.05, false discovery rate corrected.

3.4. ROI-based intrinsic FC

To further explore age-related differences in RSFC within and between the default and dorsal attention networks, we analyzed RSFC between pairs and sets of critical nodes of these 2 networks as described in the task-based ROI analysis previously mentioned. Fig. 6 displays the contrast between the young versus older adults' full correlation matrices of every node of the default and dorsal attention networks with every other node for both the GSR + Scrubbing and ANATICOR analyses. Older adults showed a robust and consistent pattern of network dedifferentiation, with reduced within-network RSFC (cool colors) of both the default network (lower-right quadrant) and dorsal attention network (upper-left quadrant), and conversely, increased RSFC (warm colors) between multiple nodes only across these 2 networks (lower-left/upper-right quadrants). Moreover, the older adults showed reduced RSFC of the MTL node with all other nodes of both the default and dorsal attention networks (yellow outline). To quantify these differences in the ANATICOR data first, a series of analysis of variance (ANOVAs) were conducted: age (young vs. older) was a between-subjects factor; differentiation (within- vs. between-network RSFC) and network (default vs. dorsal attention) were within-subject factors. Because the MTL node showed a unique pattern of RSFC, and because its' fundamental status as a default network region is questionable (see previously mentioned), the MTL node was excluded from the network-level analyses. First, a 3-way ANOVA with age (young vs. older) as a between-subjects factor, differentiation (within- vs. between-network RSFC), and network (default vs. dorsal attention) as within-subjects factors revealed a significant main effect of age ($F_{1,113} = 12.42$, $p < 0.001$), differentiation ($F_{1,113} = 528.39$, $p < 0.001$), and most important, a significant age by differentiation crossover interaction ($F_{1,113} = 32.49$, $p < 0.001$). Notably, there was no significant 3-way interaction (age × differentiation × network: $F_{1,113} = 0.12$, $p = 0.73$) indicating that this age-related dedifferentiation was not significantly different between the 2 networks. Analyses of each network and each node individually demonstrated that this pattern of age-related dedifferentiation characterized both networks individually, with significant main effects of age (default: $F_{1,113} = 11.40$, $p < 0.001$; dorsal attention: $F_{1,113} = 9.12$, $p < 0.005$), differentiation (default: $F_{1,113} = 354.90$, $p < 0.001$; dorsal attention: $F_{1,113} = 431.47$, $p < 0.001$), and age by differentiation crossover interactions (default: $F_{1,113} = 23.63$, $p < 0.001$; dorsal attention: $F_{1,113} = 24.43$, $p < 0.001$); and most of the individual nodes of both networks as well (see Table 1 for a full list of all significant interactions). The same analyses with the GSR + Scrubbing data showed a highly consistent pattern of results (see Table 1). Finally, a 2-way ANOVA demonstrated that the MTL ROI showed reduced RSFC across both networks, with a main effect of age ($F_{1,113} = 178.18$, $p < 0.001$), but notably, no age by differentiation interaction ($F_{1,113} = 0.70$, $p = 0.40$) indicating that the MTL showed a parallel reduction in RSFC with both the default and dorsal attention networks in the older adults.

4. Discussion

Anticorrelation between low-frequency BOLD signal fluctuations in the dorsal attention and default networks is a robust
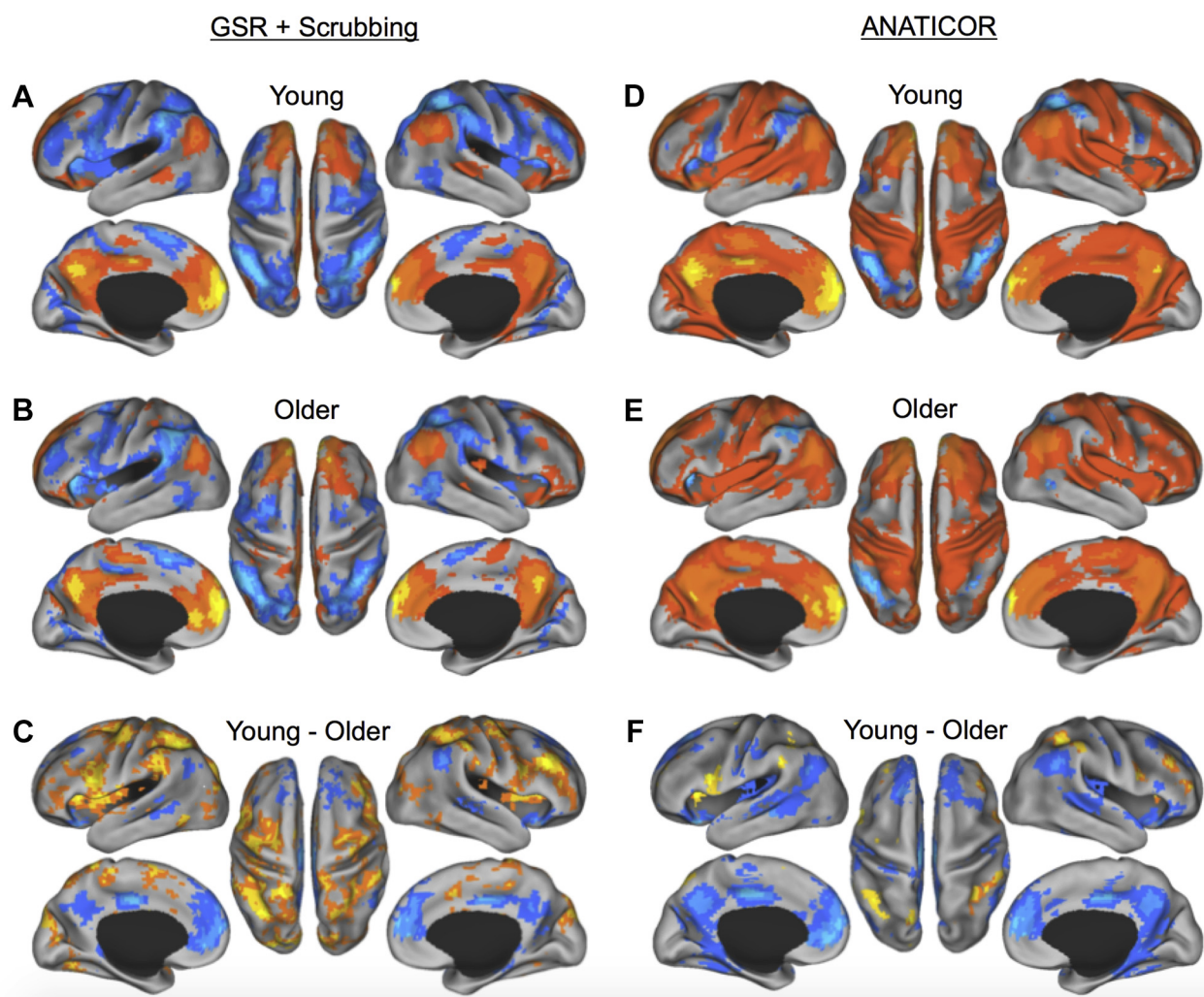
Fig. 4. RSFC of the MPFC in young versus older adults using GRS + Scrubbing (A–C) and ANATICOR (D–F). (A and D) In young adults, the MPFC shows positive RSFC with other regions of the default network (warm colors), and negative RSFC with only dorsal attention network regions (cool colors). (B and E) In older adults, the MPFC shows reduced RSFC with other regions of the default network (warm colors) and reduced anticorrelations with dorsal attention network regions (cool colors). (C and F) Contrast of young versus older adults. In older adults, the MPFC shows reduced RSFC with other regions of the default network (cool colors), but increased RSFC with regions of the dorsal attention network (warm colors), relative to young adults. $p < 0.05$; false discovery rate corrected. Abbreviations: MPFC, medial prefrontal cortex; RSFC, resting-state FC. (For interpretation of the references to color in this figure legend, the reader is referred to the Web version of this article.)

feature of the functional network architecture of the brain (Chai et al., 2012; Fox et al., 2005, 2009; Fransson, 2005; Kelly et al., 2008; Kundu et al., 2013). Here, we were able to replicate this pattern in young adults during a task known to engage the default network and during rest. Critically, we also demonstrated that anticorrelation between the dorsal attention and default networks is attenuated in older adults. This pattern is consistent across both task and resting-state conditions. During an autobiographical planning task, activity within the MPFC, a critical default network node, was positively correlated with other default network regions, and anticorrelated with regions of the dorsal attention network in younger adults. In older adults, task-related MPFC activity was functionally coupled with regions of both the default network, and key regions of the dorsal attention network, including FEF, MT+, IPS, SPL, and DLPFC (Fig. 2).

RSFC analyses, which critically did not involve GSR, revealed an age-related pattern of reduced anticorrelation that closely overlapped with the task-based results. RSFC of MPFC and PCC seed regions revealed a more robust pattern of connectivity with other default network regions for younger versus older adults, consistent

with previous reports (e.g., Andrews-Hanna et al., 2007; Damoiseaux et al., 2008). Furthermore, default network regions showed reliable anticorrelations with dorsal attention regions, including FEF, PrCv, MT+, IPS, SPL, and DLPFC, in young. In contrast, older adults demonstrated greater correlations between default and dorsal attention network regions. Interregional RSFC between robustly validated network ROIs of the default and dorsal attention networks replicated this pattern. Age-related decreases within both the dorsal attention and default networks were observed in the context of increased between-network connectivity for older adults. These findings provide strong evidence, converging across both task and rest, that reduced anticorrelation between default and dorsal attention networks is a core feature of age-related functional brain change. Furthermore, the MTL—a critical region known to show age-related declines in structure and function which may underlie age-related declines in memory (Grady, 2012)—had reduced intrinsic FC with both the dorsal attention and default networks in older adults, potentially reflecting a fractionation of the MTL memory system from other large-scale cortical networks in aging.
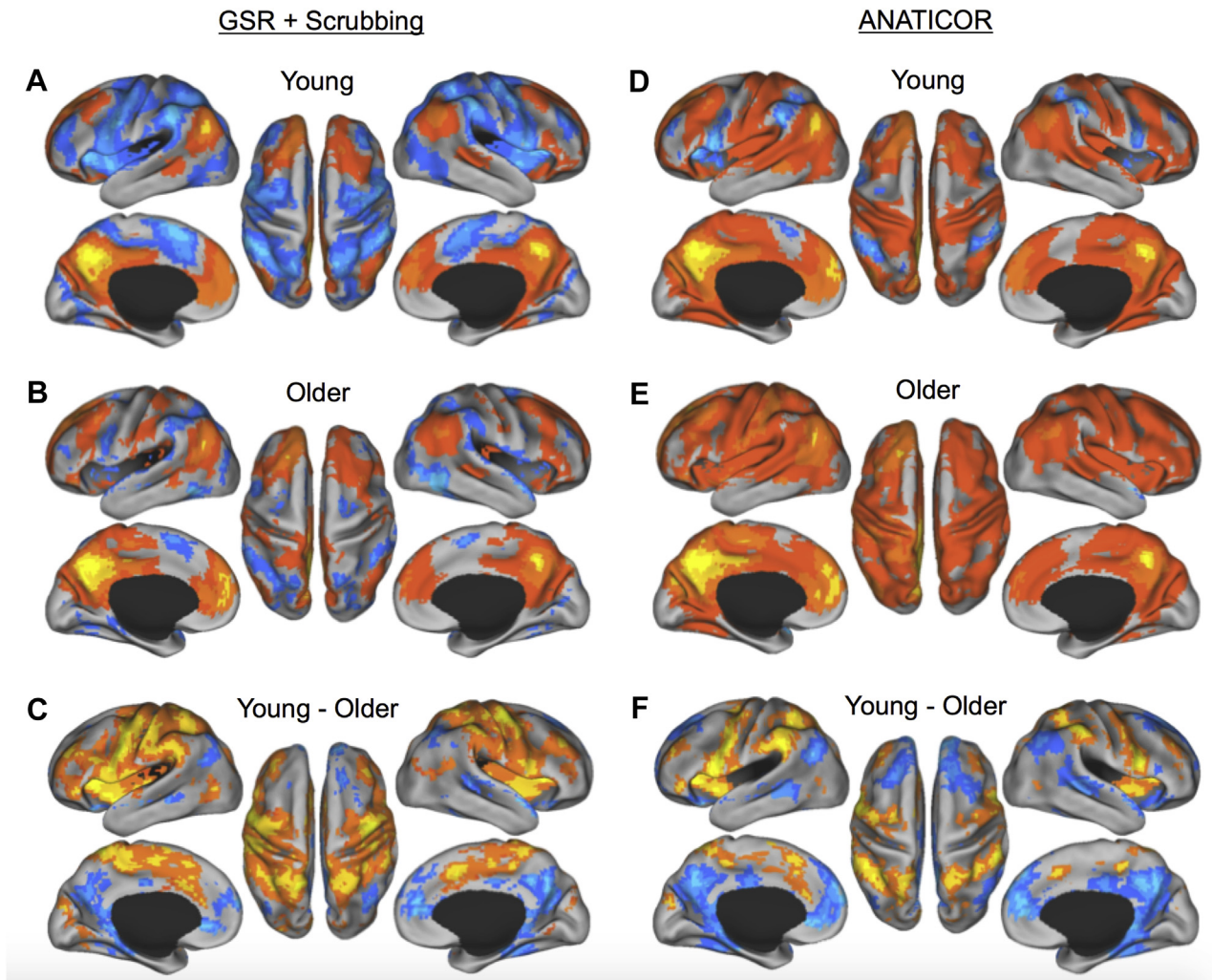
Fig. 5. RSFC of the PCC in young versus older adults using GRS + Scrubbing (A–C) and ANATICOR (D–F). (A and D) In young adults, the PCC shows positive RSFC with other regions of the default network (warm colors), and negative RSFC with only dorsal attention network regions (cool colors). (B and E) In older adults, the PCC shows reduced RSFC with other regions of the default network (warm colors) and reduced anticorrelations with dorsal attention network regions (cool colors). (C and F) Contrast of young versus older adults. In older adults, the PCC shows reduced RSFC with other regions of the default network (cool colors), but increased RSFC with regions of the dorsal attention network (warm colors), relative to young adults. $p < 0.05$; false discovery rate corrected. Abbreviations: PCC, posterior cingulate cortex; RSFC, resting-state FC. (For interpretation of the references to color in this figure legend, the reader is referred to the Web version of this article.)

4.1. Age-related changes in functional network architecture

Although few studies have directly investigated age-related changes in network anticorrelations, reductions in whole-brain functional segregation, or network modularity, have been reported (Betzel et al., 2014; Chan et al., 2014; Geerligs et al., 2014, 2015; Meunier et al., 2009; Onoda and Yamaguchi, 2013; Song et al., 2014). Age-related changes have also been investigated within specific functional networks. Grady et al. (2016) showed that increased FC between the frontoparietal control and default networks predicted reduced connectivity within the default network and better performance on cognitive measures. Spreng and Schacter (2012) reported reduced flexibility in the coupling of default and frontoparietal control network regions during shifts from internally to externally directed attention in older relative to young adults. With greater task challenge on a Tower of London planning task, greater lateral PFC coupling with the default network was observed in older adults (Turner and Spreng, 2015).

There is increasing evidence that altered network dynamics, whether at the level of the whole-brain, or among specific networks, is a central feature of brain aging. Yet few studies have investigated age-related changes in the pattern of anticorrelation between default and dorsal attention networks, one of the most robust features of the brain's functional architecture in young adults. Increased correlations and reduced anticorrelations have been reported for both whole brain (Betzel et al., 2014) and in more targeted analyses (Wu et al., 2011). However, these studies incorporated GSR as part of their RSFC data preprocessing making it difficult to reliably interpret patterns of negative and positive correlations (Gotts et al., 2013; Murphy et al., 2009; Saad et al., 2012). Chan et al. (2014) observed increased FC between default and dorsal attention brain regions with increasing age, although they excluded negative correlations from their analyses owing to concerns with GSR. More recently, reduced anticorrelations, limited to regions of medial and lateral prefrontal cortex, were observed in older versus younger adults during rest (Keller et al., 2015). Greater anticorrelation between MPFC and lateral PFC brain regions was associated with better cognitive performance in young adults; however, no behavioral associations were observed in older adults leaving the question open as to whether changes to the anticorrelation dynamic indicate age-related cognitive decline.
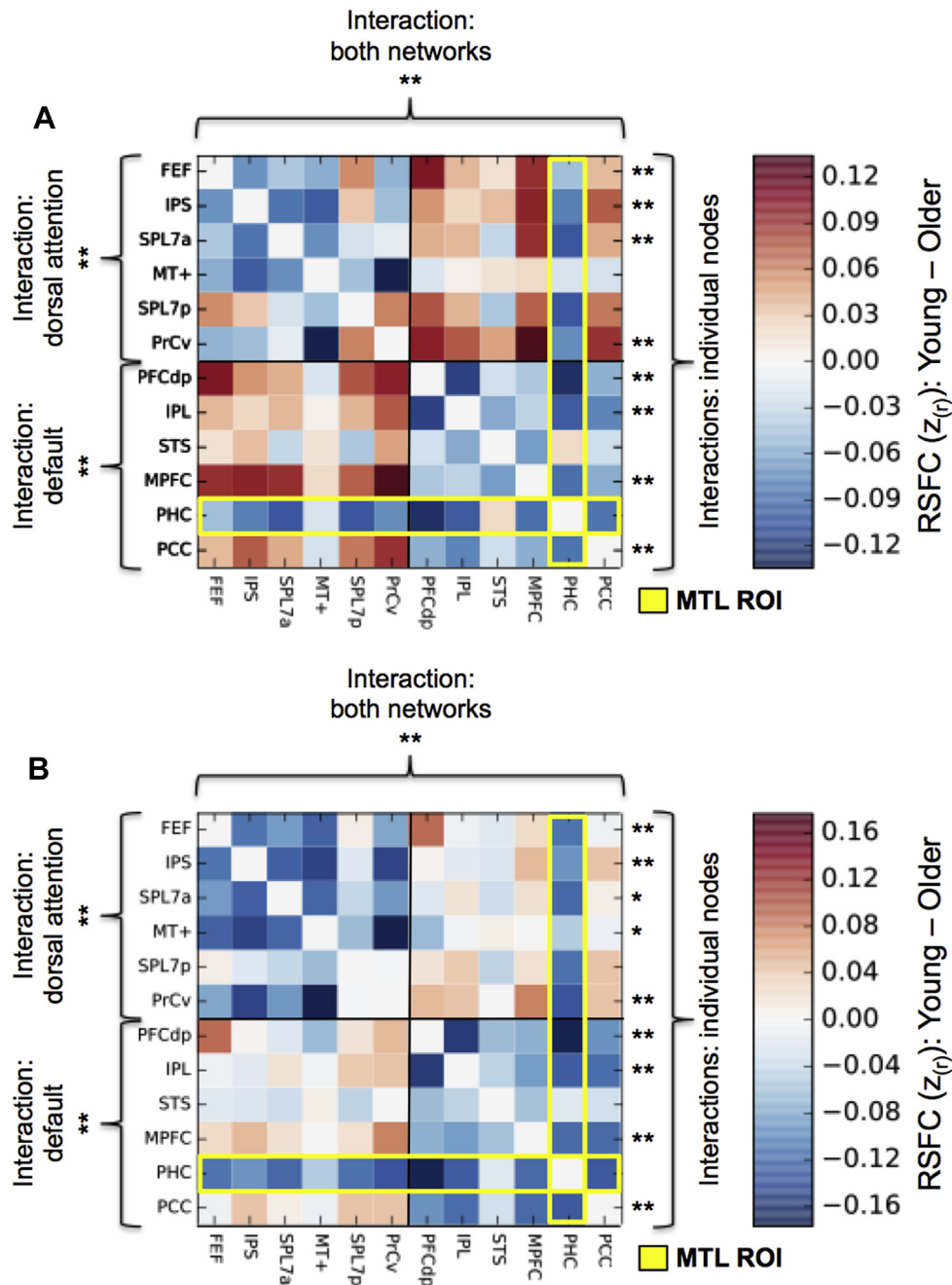
Fig. 6. Dedifferentiation of the default and dorsal attention networks in older adults. (A) GSR + Scrubbing. (B) ANATICOR. Contrasting the full correlation matrix of all ROIs of the default and dorsal attention networks for young versus older adults demonstrates reduced (cool colors) within-network RSFC of both the default and dorsal attention networks, and increased (warm colors) between-network RSFC in older adults. Significant age (young vs. older) × differentiation (within- vs. between-network RSFC) interactions were observed for RSFC when collapsed across both networks (top), for each network individually (left), and for the majority of individual ROIs of both networks (right). The MTL ROI (para-hippocampal cortex; yellow outline) showed reduced RSFC with all other ROIs across both networks in older relative to young adults. **significant crossover interaction; *significant interaction. The findings are consistent across preprocessing procedures. See Table 1 for F-statistics, p-values, node labels, and node coordinates. Abbreviations: FEF, frontal eye fields; GSR, global signal regression; IPL, inferior parietal lobule; IPS, inferior parietal sulcus; MPFC, medial prefrontal cortex; MT+, middle temporal area complex; MTL, medial temporal lobe; PFCdp, posterior dorsolateral prefrontal cortex; PCC, posterior cingulate cortex; PrCv, ventral precentral sulcus; ROI, regions of interest; RSFC, resting-state FC; SPL7a, anterior superior parietal lobule; SPL7p, posterior superior parietal lobule; STS, superior temporal sulcus. (For interpretation of the references to color in this figure legend, the reader is referred to the Web version of this article.)

Our results extend these earlier findings in 3 critical aspects. First, we demonstrate convergent patterns of reduced default-dorsal attention anticorrelations during both task and rest. Second, we show reduced anticorrelation during a task that is known to activate the default network similarly in both young and older adults, enabling us to distinguish age-related differences in connectivity in the context of matched levels of task-related activation, as opposed to in resting-state. Furthermore, we show reduced anticorrelation during the resting state without using GSR, thereby avoiding the introduction of spurious negative correlations. Finally, we show a striking reduction of intrinsic FC of the MTL with both the dorsal attention and default networks.

4.2. Reduced anticorrelations during both task and rest

The patterns of age-related reductions in anticorrelation between dorsal attention and default networks observed during task and rest are strikingly consistent (see Figs. 3 and 6). The correspondence across analysis methods provides strong support for our prediction that reduced anticorrelation between default and dorsal attention brain regions is a fundamental component of network dedifferentiation in aging (cf. Chan et al., 2014; Geerligs et al., 2015). Strong coherence in functional network architecture between task and rest has been reported previously (Smith et al., 2009; Spreng et al., 2013). From this perspective, age-related changes in the brain's intrinsic network architecture, including the increased default and dorsal attention coupling observed here, may represent a continuous sculpting of these network interactions across the lifespan in response to, or perhaps leading to, lifespan changes in cognitive functioning (see Stevens and Spreng, 2014, for a review). Increased functional coupling between default and dorsal attention network regions in older adults may be attributable to sustained task effects, with older adults attending more to externally presented stimuli during autobiographical planning. Reduced anticorrelation, or increased connectivity between the default and dorsal attention networks in older adulthood, is consistent with poor modulation of attentional processes and their neural substrates in response to shifting cognitive demands in older adults (Clapp et al., 2011; Turner and Spreng, 2012).

4.3. Reduced default-dorsal attention network anticorrelation during task

Task by age-group interactions have been widely observed within the dorsal attention network using fMRI (also referred to as the "task-positive" network—reviewed by Spreng et al., 2010b) and the default network (reviewed by Hafkemeijer et al., 2012). However, few studies have examined changes in default network activity during internally oriented tasks such as the autobiographical task used here. In a previous report, we observed no age differences in the activation of the default network during autobiographical planning, although the design was sufficiently powered to detect differences in Tower of London planning task performance in the same sample (Spreng and Schacter, 2012, Fig. 1). Here, we did observe an age-related difference in connectivity patterns between a key region of the default network, MPFC, and dorsal attention network regions during autobiographical planning (Fig. 2). The autobiographical planning task enabled us to observe FC changes in older adults during a task known to engage the default network, thereby eliminating the potential confound of age-differences in task-based activations.

4.4. Reduced default-dorsal attention network anticorrelation during rest

Numerous prior studies have shown reduced connectivity within the default network during rest (Andrews-Hanna et al., 2007; Damoiseaux et al., 2008; Grady et al., 2012; Hampson et al., 2012; Meier et al., 2012; Mevel et al., 2013; Onoda et al., 2012; Sala-Llonch et al., 2012; Saverino et al., 2015). As previously mentioned, studies also report altered connectivity between default and other brain networks (Betzel et al., 2014; Chan et al., 2014; Geerligs et al., 2015; Keller et al., 2015; Meunier et al., 2009; Wu et al., 2011). Few studies have investigated anticorrelations, as negative correlations are often discarded from analysis due to confounds related to GSR (e.g., Chan et al., 2014). The biological meaning of anticorrelations is still unclear. In healthy younger adults, the magnitude of anticorrelation has been linked to individual differences in task performance (Hampson et al., 2010; Keller et al., 2015; Kelly et al., 2008). However, the behavioral implications of reduced anticorrelation for older adults remain unclear. Future work is required to elucidate the cognitive implications of the lifespan changes in interactions amongst large-scale functional brain networks (Onoda et al., 2012). Changes in the competitive relationship between the default and dorsal attention networks from younger to older adulthood, as we describe here, will need to be further explored in tandem with sufficient denoising approaches (e.g., Chai et al., 2012; Jo et al., 2013; Kundu et al., 2012) that allow for the valid interpretation of negative correlation differences between groups (Gotts et al., 2013; Saad et al., 2012). Alternate methods are emerging, which allow for an unconfounded assessment of anticorrelations, including anatomical CompCor (Behzadi et al., 2007), temporal CompCor (Behzadi et al., 2007), or the median angle shift approach (He and Liu, 2012).

A striking finding of this study was the substantially reduced RSFC of the MTL with almost all critical nodes of both the dorsal attention and default networks. Previous work provides evidence that the MTL memory system may have a unique functional relationship with the default network: first, subregions of the MTL show dissociable patterns of FC with different cortical networks (Kahn et al., 2008; Vincent et al., 2006), which are differentially affected by aging (Das et al., 2013, 2015). Second, using 2 different frequencies of transcranial magnetic stimulation to the same default network node in the IPL, Eldaief et al. (2011) demonstrated distinct changes in FC strength among default network nodes, such that low-frequency stimulation modulates FC of IPL with the MTL but no other default network nodes, and conversely, high-frequency simulation altered FC of the IPL with other default network nodes but not the MTL. These results demonstrate that at least 2 distinct subsystems exist, dissociating the MTL from other default network regions. Finally, Ward et al. (2014) demonstrated that the MTL memory system is indirectly functionally connected to the default network via the posterior parahippocampal gyrus—the same MTL default network region investigated in the present study—demonstrating that this default network node may be the critical connection point linking the MTL memory system to the default network, a critical interaction required for episodic memory and prospection (Addis et al., 2007; Benoit and Schacter, 2015; Schacter et al., 2007). Whereas a previous study failed to find age-related differences in FC of the MTL subsystem of the default network, despite changes in all other default network subsystems (Campbell et al., 2013), here we find a robust decline in FC of the MTL with all other nodes of the default network investigated. Moreover, the age-related decline in FC was not limited to the default network but was also apparent for FC with the dorsal attention network. Given the critical role of the posterior parahippocampal cortex in linking the MTL memory system with the default network, these results suggest a potential fractionation of the MTL memory system from other large-scale networks in typical nonpathological aging. This observation is consistent with a recent report of reduced MTL-cortical connectivity where the hippocampus becomes more functionally isolated (Salami et al., 2014). Future research will be needed to explore this intriguing possibility further, including FC with other brain networks as well.

4.5. Conclusion

The functional network architecture of the human brain undergoes significant changes across the adult lifespan, transitioning from a highly modular structure to a less segregated, or dedifferentiated, network architecture. A central feature of functional segregation in younger adults is a robust pattern of anticorrelated brain activity between dorsal attention and default

network brain regions. Yet little was known about how this anticorrelated pattern of brain activity might change with age. Here, we demonstrate that anticorrelations between default and dorsal attention networks are reduced in older adults. Furthermore, this pattern is highly consistent both during task performance and at rest. As anticorrelation between these networks is associated with cognitive function in young, mapping the trajectory of age-related changes in anticorrelations between dorsal attention and default networks may provide an important marker of age-related changes to cognition. Finally, our results suggest a fractionation of the MTL memory system from other large-scale brain networks, which may underlie episodic memory decline, a hallmark of both typical healthy and pathological neurocognitive aging.

Disclosure statement

The authors report no actual or potential conflicts of interest.

Acknowledgements

Appendix A. Supplementary data

Supplementary data associated with this article can be found, in the online version, at http://dx.doi.org/10.1016/j.neurobiolaging.2016.05.020.

References

Addis, D.R., Wong, A.T., Schacter, D.L., 2007. Remembering the past and imagining the future: common and distinct neural substrates during event construction and elaboration. Neuropsychologia 45, 1363–1377.

Andrews-Hanna, J.R., Snyder, A.Z., Vincent, J.L., Lustig, C., Head, D., Raichle, M.E., Buckner, R.L., 2007. Disruption of large-scale brain systems in advanced aging. Neuron 56, 924–935.

Behzadi, Y., Restom, K., Liau, J., Liu, T.T., 2007. A component based noise correction method (CompCor) for BOLD and perfusion based fMRI. Neuroimage 37, 90–101.

Benoit, R.G., Schacter, D.L., 2015. Specifying the core network supporting episodic simulation and episodic memory by activation likelihood estimation. Neuropsychologia 75, 450–457.

Betzel, R.F., Byrge, L., He, Y., Goni, J., Zuo, X.N., Sporns, O., 2014. Changes in structural and functional connectivity among resting-state networks across the human lifespan. Neuroimage 102, 345–357.

Buckner, R.L., Head, D., Parker, J., Fotenos, A.F., Marcus, D., Morris, J.C., Snyder, A.Z., 2004. A unified approach for morphometric and functional data analysis in young, old, and demented adults using automated atlas-based head size normalization: reliability and validation against manual measurement of total intracranial volume. Neuroimage 23, 724–738.

Campbell, K.L., Grigg, O., Saverino, C., Churchill, N., Grady, C.L., 2013. Age differences in the intrinsic functional connectivity of default network subsystems. Front Aging Neurosci. 5, 73.

Chai, X.J., Castanon, A.N., Ongur, D., Whitfield-Gabrieli, S., 2012. Anticorrelations in resting state networks without global signal regression. Neuroimage 59, 1420–1428.

Chan, M.Y., Park, D.C., Savalia, N.K., Petersen, S.E., Wig, G.S., 2014. Decreased segregation of brain systems across the healthy adult lifespan. Proc. Natl. Acad. Sci. U S A 111, E4997–E5006.

Clapp, W.C., Rubens, M.T., Sabharwal, J., Gazzaley, A., 2011. Deficit in switching between functional brain networks underlies the impact of multitasking on working memory in older adults. Proc. Natl. Acad. Sci. U S A 108, 7212–7217.

Cox, R.W., 1996. AFNI: software for analysis and visualization of functional magnetic resonance neuroimages. Comput. Biomed. Res. 29, 162–173.

Damoiseaux, J.S., Beckmann, C.F., Arigita, E.J., Barkhof, F., Scheltens, P., Stam, C.J., Smith, S.M., Rombouts, S.A., 2008. Reduced resting-state brain activity in the "default network" in normal aging. Cereb. Cortex 18, 1856–1864.

Das, S.R., Pluta, J., Mancuso, L., Kliot, D., Orozco, S., Dickerson, B.C., Yushkevich, P.A., Wolk, D.A., 2013. Increased functional connectivity within medial temporal lobe in mild cognitive impairment. Hippocampus 23, 1–6.

Das, S.R., Pluta, J., Mancuso, L., Kliot, D., Yushkevich, P.A., Wolk, D.A., 2015. Anterior and posterior MTL networks in aging and MCI. Neurobiol. Aging 36, S141–S150. S150 e141.

Eldaief, M.C., Halko, M.A., Buckner, R.L., Pascual-Leone, A., 2011. Transcranial magnetic stimulation modulates the brain's intrinsic activity in a frequency-dependent manner. Proc. Natl. Acad. Sci. U S A 108, 21229–21234.

Fischl, B., Salat, D.H., Busa, E., Albert, M., Dieterich, M., Haselgrove, C., van der Kouwe, A., Killiany, R., Kennedy, D., Klaveness, S., Montillo, A., Makris, N., Rosen, B., Dale, A.M., 2002. Whole brain segmentation: automated labeling of neuroanatomical structures in the human brain. Neuron 33, 341–355.

Fox, M.D., Snyder, A.Z., Vincent, J.L., Corbetta, M., Van Essen, D.C., Raichle, M.E., 2005. The human brain is intrinsically organized into dynamic, anticorrelated functional networks. Proc. Natl. Acad. Sci. U S A 102, 9673–9678.

Fox, M.D., Zhang, D., Snyder, A.Z., Raichle, M.E., 2009. The global signal and observed anticorrelated resting state brain networks. J. Neurophysiol. 101, 3270–3283.

Fransson, P., 2005. Spontaneous low-frequency BOLD signal fluctuations: an fMRI investigation of the resting-state default mode of brain function hypothesis. Hum. Brain Mapp. 26, 15–29.

Geerligs, L., Maurits, N.M., Renken, R.J., Lorist, M.M., 2014. Reduced specificity of functional connectivity in the aging brain during task performance. Hum. Brain Mapp. 35, 319–330.

Geerligs, L., Renken, R.J., Saliasi, E., Maurits, N.M., Lorist, M.M., 2015. A brain-wide study of age-related changes in functional connectivity. Cereb. Cortex 25, 1987–1999.

Golland, Y., Golland, P., Bentin, S., Malach, R., 2008. Data-driven clustering reveals a fundamental subdivision of the human cortex into two global systems. Neuropsychologia 46, 540–553.

Gotts, S.J., Saad, Z.S., Jo, H.J., Wallace, G.L., Cox, R.W., Martin, A., 2013. The perils of global signal regression for group comparisons: a case study of Autism Spectrum Disorders. Front Hum. Neurosci. 7, 356.

Grady, C., 2012. The cognitive neuroscience of ageing. Nat. Rev. Neurosci. 13, 491–505.

Grady, C., Sarraf, S., Saverino, C., Campbell, K., 2016. Age differences in the functional interactions among the default, frontoparietal control, and dorsal attention networks. Neurobiol. Aging 41, 159–172.

Grady, C.L., Grigg, O., Ng, C., 2012. Age differences in default and reward networks during processing of personally relevant information. Neuropsychologia 50, 1682–1697.

Grady, C.L., Protzner, A.B., Kovacevic, N., Strother, S.C., Afshin-Pour, B., Wojtowicz, M., Anderson, J.A., Churchill, N., McIntosh, A.R., 2010. A multivariate analysis of age-related differences in default mode and task-positive networks across multiple cognitive domains. Cereb. Cortex 20, 1432–1447.

Gusnard, D.A., Raichle, M.E., Raichle, M.E., 2001. Searching for a baseline: functional imaging and the resting human brain. Nat. Rev. Neurosci. 2, 685–694.

Hafkemeijer, A., van der Grond, J., Rombouts, S.A., 2012. Imaging the default mode network in aging and dementia. Biochim. Biophys. Acta 1822, 431–441.

Hampson, M., Driesen, N., Roth, J.K., Gore, J.C., Constable, R.T., 2010. Functional connectivity between task-positive and task-negative brain areas and its relation to working memory performance. Magn. Reson. Imaging 28, 1051–1057.

Hampson, M., Tokoglu, F., Shen, X., Scheinost, D., Papademetris, X., Constable, R.T., 2012. Intrinsic brain connectivity related to age in young and middle aged adults. PLoS One 7, e44067.

He, H., Liu, T.T., 2012. A geometric view of global signal confounds in resting-state functional MRI. Neuroimage 59, 2339–2348.

Jin, M., Pelak, V.S., Cordes, D., 2012. Aberrant default mode network in subjects with amnestic mild cognitive impairment using resting-state functional MRI. Magn. Reson. Imaging 30, 48–61.

Jo, H.J., Gotts, S.J., Reynolds, R.C., Bandettini, P.A., Martin, A., Cox, R.W., Saad, Z.S., 2013. Effective preprocessing procedures virtually eliminate distance-dependent motion artifacts in resting state fMRI. J. Appl. Math 1–9. http://dx.doi.org/10.1155/2013/935154.

Jo, H.J., Saad, Z.S., Simmons, W.K., Milbury, L.A., Cox, R.W., 2010. Mapping sources of correlation in resting state FMRI, with artifact detection and removal. Neuroimage 52, 571–582.

Kahn, I., Andrews-Hanna, J.R., Vincent, J.L., Snyder, A.Z., Buckner, R.L., 2008. Distinct cortical anatomy linked to subregions of the medial temporal lobe revealed by intrinsic functional connectivity. J. Neurophysiol. 100, 129–139.

Keller, J.B., Hedden, T., Thompson, T.W., Anteraper, S.A., Gabrieli, J.D., Whitfield-Gabrieli, S., 2015. Resting-state anticorrelations between medial and lateral prefrontal cortex: association with working memory, aging, and individual differences. Cortex 64, 271–280.

Kelly, A.M., Uddin, L.Q., Biswal, B.B., Castellanos, F.X., Milham, M.P., 2008. Competition between functional brain networks mediates behavioral variability. Neuroimage 39, 527–537.

Krishnan, A., Williams, L.J., McIntosh, A.R., Abdi, H., 2011. Partial Least Squares (PLS) methods for neuroimaging: a tutorial and review. Neuroimage 56, 455–475.

Kundu, P., Brenowitz, N.D., Voon, V., Worbe, Y., Vertes, P.E., Inati, S.J., Saad, Z.S., Bandettini, P.A., Bullmore, E.T., 2013. Integrated strategy for improving functional connectivity mapping using multiecho fMRI. Proc. Natl. Acad. Sci. U S A 110, 16187–16192.

Kundu, P., Inati, S.J., Evans, J.W., Luh, W.M., Bandettini, P.A., 2012. Differentiating BOLD and non-BOLD signals in fMRI time series using multi-echo EPI. Neuroimage 60, 1759–1770.

McIntosh, A.R., 1999. Mapping cognition to the brain through neural interactions. Memory 7, 523—548.

Meier, T.B., Desphande, A.S., Vergun, S., Nair, V.A., Song, J., Biswal, B.B., Meyerand, M.E., Birn, R.M., Prabhakaran, V., 2012. Support vector machine classification and characterization of age-related reorganization of functional brain networks. Neuroimage 60, 601—613.

Meunier, D., Achard, S., Morcom, A., Bullmore, E., 2009. Age-related changes in modular organization of human brain functional networks. Neuroimage 44, 715—723.

Mevel, K., Chételat, G., Eustache, F., Desgranges, B., 2011. The default mode network in healthy aging and Alzheimer's disease. Int. J. Alzheimers Dis. 2011, 535816.

Mevel, K., Landeau, B., Fouquet, M., La Joie, R., Villain, N., Mézenge, F., Perrotin, A., Eustache, F., Desgranges, B., Chételat, G., 2013. Age effect on the default mode network, inner thoughts, and cognitive abilities. Neurobiol. Aging 34, 1292—1301.

Murphy, K., Birn, R.M., Handwerker, D.A., Jones, T.B., Bandettini, P.A., 2009. The impact of global signal regression on resting state correlations: are anti-correlated networks introduced? Neuroimage 44, 893—905.

Onoda, K., Ishihara, M., Yamaguchi, S., 2012. Decreased functional connectivity by aging is associated with cognitive decline. J. Cogn. Neurosci. 24, 2186—2198.

Onoda, K., Yamaguchi, S., 2013. Small-worldness and modularity of the resting-state functional brain network decrease with aging. Neurosci. Lett. 556, 104—108.

Power, J.D., Barnes, K.A., Snyder, A.Z., Schlaggar, B.L., Petersen, S.E., 2012. Spurious but systematic correlations in functional connectivity MRI networks arise from subject motion. Neuroimage 59, 2142—2154.

Power, J.D., Mitra, A., Laumann, T.O., Snyder, A.Z., Schlaggar, B.L., Petersen, S.E., 2014. Methods to detect, characterize, and remove motion artifact in resting state fMRI. Neuroimage 84, 320—341.

Saad, Z.S., Gotts, S.J., Murphy, K., Chen, G., Jo, H.J., Martin, A., Cox, R.W., 2012. Trouble at rest: how correlation patterns and group differences become distorted after global signal regression. Brain Connect 2, 25—32.

Sala-Llonch, R., Arenaza-Urquijo, E.M., Valls-Pedret, C., Vidal-Pineiro, D., Bargallo, N., Junque, C., Bartrés-Faz, D., 2012. Dynamic functional re-organizations and relationship with working memory performance in healthy aging. Front Hum. Neurosci. 6, 152.

Salami, A., Pudas, S., Nyberg, L., 2014. Elevated hippocampal resting-state connectivity underlies deficient neurocognitive function in aging. Proc. Natl. Acad. Sci. U S A 111, 17654—17659.

Sambataro, F., Murty, V.P., Callicott, J.H., Tan, H.Y., Das, S., Weinberger, D.R., Mattay, V.S., 2010. Age-related alterations in default mode network: impact on working memory performance. Neurobiol. Aging 31, 839—852.

Satterthwaite, T.D., Elliott, M.A., Gerraty, R.T., Ruparel, K., Loughead, J., Calkins, M.E., Eickhoff, S.B., Hakonarson, H., Gur, R.C., Gur, R.E., Wolf, D.H., 2013. An improved framework for confound regression and filtering for control of motion artifact in the preprocessing of resting-state functional connectivity data. Neuroimage 64, 240—256.

Satterthwaite, T.D., Wolf, D.H., Loughead, J., Ruparel, K., Elliott, M.A., Hakonarson, H., Gur, R.C., Gur, R.E., 2012. Impact of in-scanner head motion on multiple measures of functional connectivity: relevance for studies of neurodevelopment in youth. Neuroimage 60, 623—632.

Saverino, C., Grigg, O., Churchill, N.W., Grady, C.L., 2015. Age differences in the default network at rest and the relation to self-referential processing. Soc. Cogn. Affect Neurosci. 10, 231—239.

Schacter, D.L., Addis, D.R., Buckner, R.L., 2007. Remembering the past to imagine the future: the prospective brain. Nat. Rev. Neurosci. 8, 657—661.

Smith, S.M., Fox, P.T., Miller, K.L., Glahn, D.C., Fox, P.M., Mackay, C.E., Filippini, N., Watkins, K.E., Toro, R., Laird, A.R., Beckmann, C.F., 2009. Correspondence of the brain's functional architecture during activation and rest. Proc. Natl. Acad. Sci. U S A 106, 13040—13045.

Song, J., Birn, R.M., Boly, M., Meier, T.B., Nair, V.A., Meyerand, M.E., Prabhakaran, V., 2014. Age-related reorganizational changes in modularity and functional connectivity of human brain networks. Brain Connect 4, 662—676.

Sperling, R.A., Dickerson, B.C., Pihlajamaki, M., Vannini, P., LaViolette, P.S., Vitolo, O.V., Hedden, T., Becker, J.A., Rentz, D.M., Selkoe, D.J., Johnson, K.A., 2010. Functional alterations in memory networks in early Alzheimer's disease. Neuromolecular Med. 12, 27—43.

Spreng, R.N., Schacter, D.L., 2012. Default network modulation and large-scale network interactivity in healthy young and old adults. Cereb. Cortex 22, 2610—2621.

Spreng, R.N., Sepulcre, J., Turner, G.R., Stevens, W.D., Schacter, D.L., 2013. Intrinsic architecture underlying the relations among the default, dorsal attention, and frontoparietal control networks of the human brain. J. Cogn. Neurosci. 25, 74—86.

Spreng, R.N., Stevens, W.D., Chamberlain, J.P., Gilmore, A.W., Schacter, D.L., 2010a. Default network activity, coupled with the frontoparietal control network, supports goal-directed cognition. Neuroimage 53, 303—317.

Spreng, R.N., Wojtowicz, M., Grady, C.L., 2010b. Reliable differences in brain activity between young and old adults: a quantitative meta-analysis across multiple cognitive domains. Neurosci. Biobehav. Rev. 34, 1178—1194.

Squire, L.R., Stark, C.E., Clark, R.E., 2004. The medial temporal lobe. Annu Rev Neurosci 27, 279—306.

Stevens, W.D., Hasher, L., Chiew, K.S., Grady, C.L., 2008. A neural mechanism underlying memory failure in older adults. J. Neurosci. 28, 12820—12824.

Stevens, W.D., Spreng, R.N., 2014. Resting-state functional connectivity MRI reveals active processes central to cognition. Wiley Interdiscip. Rev. Cogn. Sci. 5, 233—245.

Stevens, W.D., Tessler, M.H., Peng, C.S., Martin, A., 2015. Functional connectivity constrains the category-related organization of human ventral occipitotemporal cortex. Hum. Brain Mapp. 36, 2187—2206.

Turner, G.R., Spreng, R.N., 2012. Executive functions and neurocognitive aging: dissociable patterns of brain activity. Neurobiol. Aging 33, 826.e1—826.e13.

Turner, G.R., Spreng, R.N., 2015. Prefrontal engagement and reduced default network suppression co-occur and are dynamically coupled in older adults: the default-executive coupling hypothesis of aging. J. Cogn. Neurosci. 27, 2462—2476.

Van Dijk, K.R., Hedden, T., Venkataraman, A., Evans, K.C., Lazar, S.W., Buckner, R.L., 2010. Intrinsic functional connectivity as a tool for human connectomics: theory, properties, and optimization. J. Neurophysiol. 103, 297—321.

Van Dijk, K.R., Sabuncu, M.R., Buckner, R.L., 2012. The influence of head motion on intrinsic functional connectivity MRI. Neuroimage 59, 431—438.

Vincent, J.L., Snyder, A.Z., Fox, M.D., Shannon, B.J., Andrews, J.R., Raichle, M.E., Buckner, R.L., 2006. Coherent spontaneous activity identifies a hippocampal-parietal memory network. J. Neurophysiol. 96, 3517—3531.

Wang, L., Zang, Y., He, Y., Liang, M., Zhang, X., Tian, L., Wu, T., Jiang, T., Li, K., 2006. Changes in hippocampal connectivity in the early stages of Alzheimer's disease: evidence from resting state fMRI. Neuroimage 31, 496—504.

Ward, A.M., Schultz, A.P., Huijbers, W., Van Dijk, K.R., Hedden, T., Sperling, R.A., 2014. The parahippocampal gyrus links the default-mode cortical network with the medial temporal lobe memory system. Hum. Brain Mapp. 35, 1061—1073.

Whitfield-Gabrieli, S., Ford, J.M., 2012. Default mode network activity and connectivity in psychopathology. Annu. Rev. Clin. Psychol. 8, 49—76.

Wu, J.T., Wu, H.Z., Yan, C.G., Chen, W.X., Zhang, H.Y., He, Y., Yang, H.S., 2011. Aging-related changes in the default mode network and its anti-correlated networks: a resting-state fMRI study. Neurosci. Lett. 504, 62—67.

Yeo, B.T., Krienen, F.M., Sepulcre, J., Sabuncu, M.R., Lashkari, D., Hollinshead, M., Roffman, J.L., Smoller, J.W., Zöllei, L., Polimeni, J.R., Fischl, B., Liu, H., Buckner, R.L., 2011. The organization of the human cerebral cortex estimated by intrinsic functional connectivity. J. Neurophysiol. 106, 1125—1165.